Soft Matter

ROYAL SOCIETY OF CHEMISTRY

PAPER

View Article Online
View Journal | View Issue

Cite this: *Soft Matter*, 2021, **17**, 3358

Changes in membrane elasticity caused by the hydrophobic surfactant proteins correlate poorly with adsorption of lipid vesicles

Ryan W. Loney,[a] Bret Brandner,[a] Maayan P. Dagan,[a] Paige N. Smith,[a] Megan Roche,[b] Jonathan R. Fritz,[b] Stephen B. Hall *[a] and Stephanie A. Tristram-Nagle *[b]

Received 18th December 2020,
Accepted 12th February 2021

DOI: 10.1039/d0sm02223c

rsc.li/soft-matter-journal

To establish how the hydrophobic surfactant proteins, SP-B and SP-C, promote adsorption of lipids to an air/water interface, we used X-ray diffuse scattering (XDS) to determine an order parameter of the lipid chains (S_{xray}) and the bending modulus of the lipid bilayers (K_C). Samples contained different amounts of the proteins with two sets of lipids. Dioleoylphosphatidylcholine (DOPC) provided a simple, well characterized model system. The nonpolar and phospholipids (N&PL) from extracted calf surfactant provided the biological mix of lipids. For both systems, the proteins produced changes in S_{xray} that correlated well with K_C. The dose–response to the proteins, however, differed. Small amounts of protein generated large decreases in S_{xray} and K_C for DOPC that progressed monotonically. The changes for the surfactant lipids were erratic. Our studies then tested whether the proteins produced correlated effects on adsorption. Experiments measured the initial fall in surface tension during adsorption to a constant surface area, and then expansion of the interface during adsorption at a constant surface tension of 40 mN m^{-1}. The proteins produced a sigmoidal increase in the rate of adsorption at 40 mN m^{-1} for both lipids. The results correlated poorly with the changes in S_{xray} and K_C in both cases. Disordering of the lipid chains produced by the proteins, and the softening of the bilayers, fail to explain how the proteins promote adsorption of lipid vesicles.

1. Introduction

Pulmonary surfactant is a mixture of lipids and proteins secreted by the type II pneumocytes of the alveolar air-sacs in the lungs. The mixture acts together as a surfactant, adsorbing to the surface of the liquid layer that lines the alveoli and forming a thin film that lowers surface tension.[1] Two hydrophobic proteins, SP-B and SP-C, are required for its function. SP-B is the only protein known to be immediately essential for pulmonary function.[2,3] Breathing in the absence of SP-B injures the lungs,[2] producing an insult equivalent to the process that occurs in premature babies who lack the complete mixture of surfactant constituents.[4] The consequences of missing SP-C are more delayed. Some familial forms of interstitial fibrosis result from abnormalities of SP-C.[5,6] Many of these disorders reflect cellular toxicity caused by misfolded forms of the precursor protein of SP-C,[7] but patients[8] and animals[9] that lack any form of SP-C also develop fibrosis. This finding suggests that the absence of SP-C may also contribute to a chronic injury during prolonged breathing with elevated alveolar surface tension. SP-B and SP-C represent minor components of pulmonary surfactant, constituting ~1.5% (w:w) of the complete mixture,[10,11] but their functional contribution is crucial.

Limited experimental access to the alveoli complicates efforts to establish how the proteins contribute to surfactant function. Studies *in vitro*, however, show that the proteins accelerate adsorption of the surfactant lipids to an air/water interface by orders of magnitude.[12,13] The most reasonable proposal concerning the function of the proteins is that they promote the rapid formation of the alveolar film.

The mechanisms by which the proteins facilitate adsorption remain poorly defined. Perhaps the simplest possibility, and certainly the earliest proposal,[14,15] is that the proteins create disorder in the surfactant lipids. The important consequence would be an increase in the flexibility of the lipid leaflets, allowing them to transform more readily from vesicular bilayers to interfacial films. The studies here used X-ray diffuse scattering (XDS) to determine if the proteins affect the order of the lipid chains and the bending modulus of the lipid bilayers. A reduction in the bending modulus would allow the lipids to reconfigure more easily from their spontaneous curvature to

[a] *Pulmonary and Critical Care Medicine, Oregon Health & Science University, Portland, Oregon 97239, USA. E-mail: sbh@ohsu.edu*
[b] *Biological Physics Group, Department of Physics, Carnegie Mellon University, Pittsburgh, Pennsylvania 15213, USA. E-mail: stn@cmu.edu*

any other structure. Our experiments first established how the proteins altered dioleoylphosphatidylcholine (DOPC), used as a simple model system, and then the complete set of surfactant lipids. We also considered the extent to which the changes detected by XDS correlate with effects of the proteins on the kinetics of adsorption.

2. Materials and methods

2.A. Materials

Dioleoylphosphatidylcholine (DOPC) was obtained from Avanti Polar Lipids (Alabaster, AL) and used without further characterization or purification. The following reagents were obtained from commercial sources: *N*-2-hydroxyethylpiperazine-*N*′-2-ethanesulfonic acid (HEPES), $CaCl_2$, chloroform, and methanol (Fischer Scientific, Hampton, NH); NaCl (Sigma, St Louis, MO). Water was filtered and photo-oxidized with ultraviolet light using a NANOpure Diamond TOC-UV water-purification system (Barnstead/Thermolyne, Dubuque, LA). The following buffers were used routinely: 10 mM HEPES at pH 7.0 and 150 mM NaCl (HS); and 10 mM HEPES at pH 7.0, 150 mM NaCl, and 1.5 mM $CaCl_2$ (HSC).

The hydrophobic constituents of calf surfactant (calf lung surfactant extract, CLSE) were provided by ONY, Inc. (Amherst, NY). CLSE represents the constituents of large aggregates collected by centrifugation of material lavaged from freshly excised calf lungs,[16] followed by extraction.[17] Gel permeation chromatography of CLSE separates the hydrophobic surfactant proteins (SPs), the phospholipids, and the non-polar lipids (cholesterol) into distinct peaks.[10,18,19] Pooling the appropriate eluted fractions provides preparations of the combined SPs or just the non-polar and phospholipids (N&PL).[10] Separation of the SPs from CLSE used a mobile phase of neutral solvent (chloroform/methanol [1 : 1 (v/v)]) to minimize esterification of the proteins.[20] Because the anionic phospholipids stick to the chromatographic column with that system,[10] we instead used an acidified solvent (chloroform/methanol/0.1 N HCl [1 : 1 : 0.05 (v/v/v)])[18] to obtain N&PL.

Concentrations of the proteins and phospholipids were determined by colorimetric assays,[21,22] using bovine serum albumin as the standard protein. The SPs contain SP-B and SP-C in a 1 : 1 weight ratio.[23] Mixtures of N&PL and CLSE varied the content of the proteins combined with the same set of surfactant lipids. The mole fraction of phospholipid contributed by CLSE in these samples, determined from the phospholipid concentration of stock solutions, was expressed as X_{CLSE} = CLSE/(N&PL + CLSE).

2.B.I. X-Ray scattering

a. Preparation of samples. Samples with DOPC were prepared by adding the combined SPs to the phospholipid. Samples containing the biological mixture of lipids combined N&PL with increasing amounts of CLSE. For samples with either DOPC or the surfactant lipids, 4 mg of material was dissolved in 200 μL of organic solvent (chloroform : methanol (3 : 1, v : v) for DOPC, and chloroform : trifluoroethanol (1 : 1, v : v) for the surfactant lipids). These mixtures were plated onto silicon wafers (15 × 1 × 30 mm) *via* the rock-and-roll method,[24] in which rocking the silicon wafer continuously during solvent evaporation produces stacks of ~1800 well-aligned bilayers. Plating occurred in a glove box (DOPC) or in a fume hood (CLSE). Once immobile, the thin film was additionally evacuated for at least 2 h. The sample was trimmed to a central 5 mm wide strip parallel to the long-edge of the wafer.[24] The vapor in a thick-walled chamber hydrated the films.[25]

b. LAXS. Low-angle X-ray scattering (LAXS) from oriented, fully hydrated samples (Fig. 1A) was obtained at the G1 line of the Cornell High Energy Synchrotron Source (CHESS, Ithaca, NY) on two separate visits using X-ray wavelengths of 1.1775 and 1.0976 Å with sample-to-detector distances of 365 and 417 mm. Measurements were carried out at 37 °C and 40 °C. Rotation of the flat silicon wafer from −1.6 to 7 degrees during the collection of data sampled all scattered X-rays equally (30 s dezingered scans). Collection of background set the X-ray angle of incidence $\omega = -2.4^\circ$, where scattering by the sample does not contribute to the image. For analysis of the data, subtraction of background first removed extraneous air and mylar scattering. Laterally symmetrizing the images increased the signal-to-noise ratio. During progressive hydration of the samples, fluctuations of the membranes produced "lobes" of diffuse scattering (Fig. 1A).[26,27] The measured fall-off of intensity in the lateral q_r direction quantitates the fluctuations. The analysis uses a non-linear least squares fit of the data to the free energy functional from liquid crystal theory,

$$f = \frac{\pi}{NL_r^2}\int r\mathrm{d}r \sum_{n=0}^{N-1}\left\{K_c\left[\nabla_r^2 u_n(r)\right]^2 + B[u_{n+1}(r) - u_n(r)]^2\right\} \quad (1)$$

where N is the number of bilayers in the Z (vertical) direction, L_r is the size of the domain in the r (horizontal) direction, K_C is the bending modulus, u_n is the vertical membrane displacement, and B is the compressibility modulus. The analysis provides K_C and B independently, where K_C describes the bending of a single bilayer;[28] a higher K_C indicates a stiffer membrane. This method has obtained bending moduli of pure lipid membranes,[29–36] and

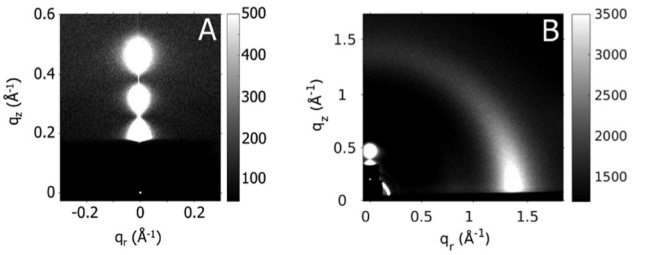

Fig. 1 XDS from oriented bilayers of N&PL/CLSE. X_{CLSE} = 0.3; temperature = 40 °C. (A) LAXS, d-spacing = 75 Å. At this greyscale, lobes of white, diffuse scattering obscure the diffracted, lamellar orders underneath. Beam appears at q_r, q_z = 0 Å^{-1} as a small, white dot through the semi-transparent, dark rectangular beam stop. (B) WAXS pattern from the same sample, with the shrunken LAXS pattern evident in the lower left-hand corner.

membranes with peptides,[37–45] cholesterol,[46–48] sugar,[49] drugs,[50] and bioflavinoids.[51]

c. WAXS. Wide-angle X-ray scattering (WAXS) was obtained during two visits to CHESS (*S*-distance = 159 and 173 mm) (Fig. 1B). The same sample that was hydrated for LAXS was X-rayed for WAXS with the CCD detector closer to the sample. Exposures were taken at two angles of X-ray incidence, $\omega = +0.5^\circ$ and $\omega = -0.5^\circ$, and then subtracted from each other. Both images were dezingered, 30 s scans. The subtraction removes extraneous scatter caused by the mylar chamber windows and shadows. The chain–chain correlation appears as diffuse scattering projected circularly upwards from the equator (Fig. 1B). The radial decrease in intensity yields information about chain order. To obtain an order parameter, S_{xray}, the intensity is first integrated along its trajectory, and then fit with wide-angle liquid crystal theory.[52] The theoretical model of chain scattering assumes long thin rods that are locally well aligned along the local director, n_L, with orientation described by the angle β. Although acyl chains from lipids in the fluid phase are not long cylinders, the model allows the cylinders to tilt at an angle, β, to approximate chain disorder. A MATLAB computer program[52] obtained S_{xray} from the fit of the intensities to eqn (2):

$$S_{xray} = \frac{1}{2}\left(3\langle\cos^2\beta\rangle - 1\right) \quad (2)$$

The program also provided the root mean square error, which indicates the quality of the fit.

2.B.II. Adsorption

a. Dispersion. Samples were generated by mixing the different constituents in chloroform. A stream of nitrogen dried the solvent to form films in test tubes. Incubation overnight at reduced pressures evaporated any remaining solvent. Samples were then hydrated overnight, and subjected to five cycles of freezing and thawing. Immediately before each experiment, bath-sonication and vortexing completed dispersion of the samples.

b. Experiments with captive bubbles. Measurements of adsorption monitored surface tension during formation of a film on a captive bubble. The shape of the bubble viewed along the horizontal axis provides its surface area and surface tension.[53–56] Each experiment began with tests for the presence of a preexisting, contaminating film. The bubble prior to introduction of the adsorbing sample had the surface tension of water within ± 2 mN m^{-1}. Compression of the bubble to roughly one-third of its initial volume changed surface tension by less than 3 mN m^{-1}. Adsorption was initiated by injecting 100 μL aliquots of concentrated vesicles prepared in HS, in which the absence of Ca^{2+} minimized fusion among vesicles, into a stirred subphase of HSC. Programs written in LabVIEW (National Instruments, Austin, TX) determined surface tension and surface area in real time.[57] A computer-driven syringe pump infused and withdrew buffer from the chamber to manipulate the bubble and hold either surface area or surface tension constant. Heating pads along the sides of the chamber maintained set temperatures.

3. Results

Measurements of adsorption by DOPC with the SPs (Fig. 2) showed behavior reported previously.[58] DOPC by itself lowered surface tension slowly. At long times of ~16 h, the process stalled when surface tension reached ~50 mN m^{-1}, which remained constant. The SPs at 0.1% increased the rate of the initial fall in surface tension, but adsorption again slowed approaching 50 mN m^{-1}. At that point, however, adsorption accelerated during a final drop to the equilibrium surface tension of ~25 mN m^{-1}. A further increase to 0.3% SP closely approximated the curves achieved with 3% protein. As demonstrated previously,[12,13,58] the proteins promoted adsorption at all surface tensions, but their effect was greatest below 50 mN m^{-1}.

Measurements of XDS investigated whether changes in the order of lipid chains and the stiffness of the lipid bilayers could explain the functional effects of the proteins. The radial variation of WAXS, which results from the chain–chain correlation, provided the order parameter for the chains, S_{xray}, analogous to the order parameter obtained by nuclear magnetic resonance. Fluctuations of the stacked bilayers, which instead determines the lateral variation of LAXS, provided the bending modulus, K_C.

The proteins produced a dose-related decrease in S_{xray} for DOPC (Fig. 3) and a corresponding drop in K_C (Fig. 4). The changes occurred with remarkably little protein. At 0.1% (w:w) protein, which is an order of magnitude below the physiological level of 1.5%, S_{xray} fell by 30% (Fig. 3). K_C decreased by 50% (Fig. 4). The changes continued to the largest amounts of protein in our samples at 3%, but particularly for K_C, most of the decrease occurred with the initial, small doses. The correspondence of changes in S_{xray} and K_C fit with disordering by the proteins causing a softening of the membranes.

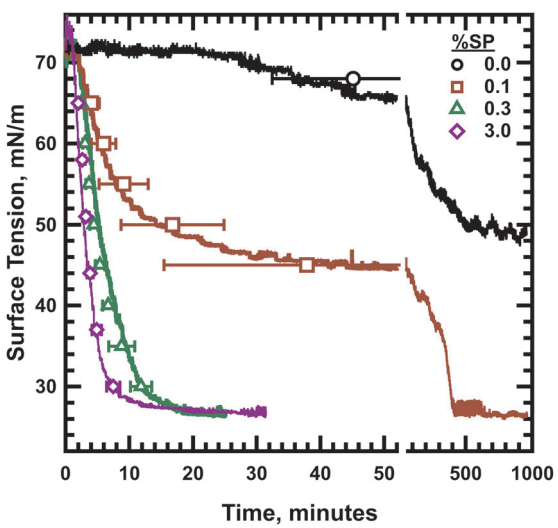

Fig. 2 Surface tension as a function of time during adsorption of SP–DOPC. Continuous traces show representative experiments that illustrate features which can be obscured during averaging. Symbols give mean time ± S.D. to reach specific surface tensions. The *x*-axis is split to show the effect of SPs at long times. Temperature = 23 °C.

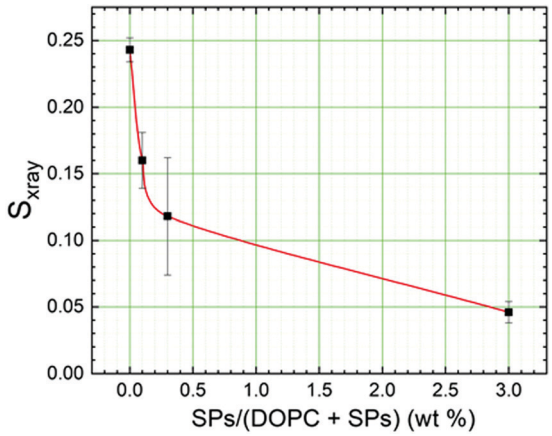

Fig. 3 Chain order parameter (S_{xray}) results for DOPC with combined SP-B and SP-C. Symbols give mean ± S.D. for duplicate or triplicate samples. The red line guides the eye. Measurements were performed at the experimentally convenient temperature of 30 °C, well above the main transition for DOPC.

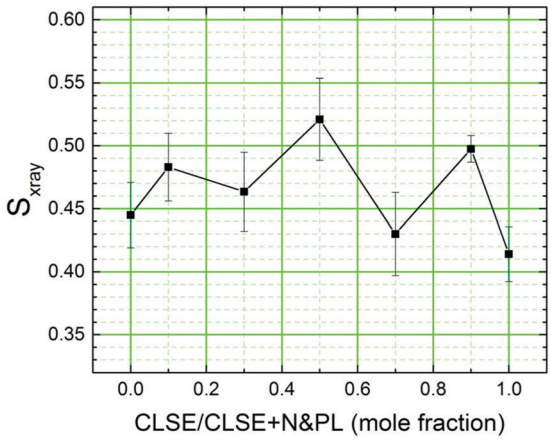

Fig. 5 S_{xray} for N&PL with added CLSE. Symbols give mean ± S.D. for duplicate or triplicate samples. Measurements were performed at 40 °C to avoid the complicating presence of the L_β phase at 37 °C.[59]

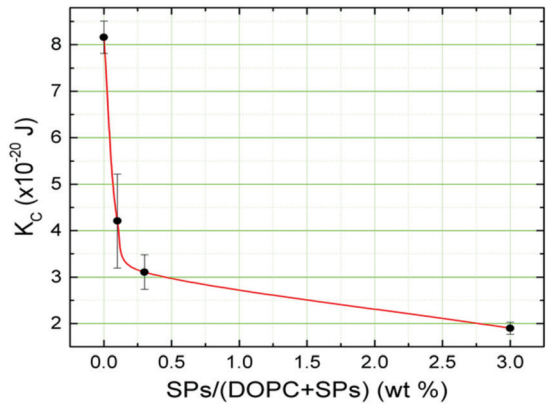

Fig. 4 Elasticity (K_C) for DOPC with the SPs. Symbols give mean ± S.D. for duplicate or triplicate samples. The red line guides the eye. Temperature = 30 °C.

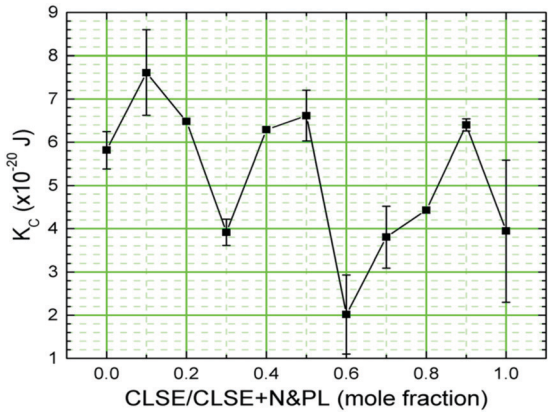

Fig. 6 K_C for N&PL/CLSE mixtures at different X_{CLSE}. Temperature = 40 °C.

To ensure that the results with DOPC extended to the biological lipids, we repeated the measurements with mixtures of N&PL and CLSE. Measurements at 37 °C and 40 °C yielded similar results. At 37 °C, coexistence of gel and fluid phases[59] complicated the analysis. We therefore only report data collected at 40 °C. These samples varied the amount of protein combined with the complete set of surfactant lipids. The measurements again showed a strong correlation of S_{xray} and K_C. Samples in which S_{xray} indicated greater chain disorder (Fig. 5) also had lower K_C values (Fig. 6), indicating a softer membrane. The dose–response to the proteins, however, was much more erratic than with DOPC, particularly for K_C (Fig. 6).

The results for S_{xray} and K_C demonstrated a disparity between the effects of the proteins on the two sets of lipids. Prior studies of adsorption, however, have suggested that the proteins similarly promote adsorption of DOPC[12,58] and the surfactant lipids.[13,58] This observation suggested that the kinetics of adsorption might correlate poorly with S_{xray} and K_C. To address this issue, we determined the dose–response of adsorption for the proteins with the two lipids.

Prior and current results (Fig. 2) indicate that the most important effects of the proteins occur during the final stages of adsorption, at surface tensions below 50 mN m^{-1}. In that stage, the fall in surface tension, which initially slows progressively, abruptly accelerates in samples containing the proteins. To quantitate adsorption in this critical lower range, our experiments let surface tension fall to 40 mN m^{-1} (Fig. 7A) during adsorption to a constant surface area. We then measured isobaric adsorption to an interface held at constant surface tension (Fig. 7B). To the extent that a given surface tension corresponds to a specific surface concentration, the change in interfacial area during isobaric measurements directly reflects molecular flux to and from the surface.[60] For samples of DOPC alone, which failed to reach a surface tension of 40 mN m^{-1} during incubation for 66 h, the rate of

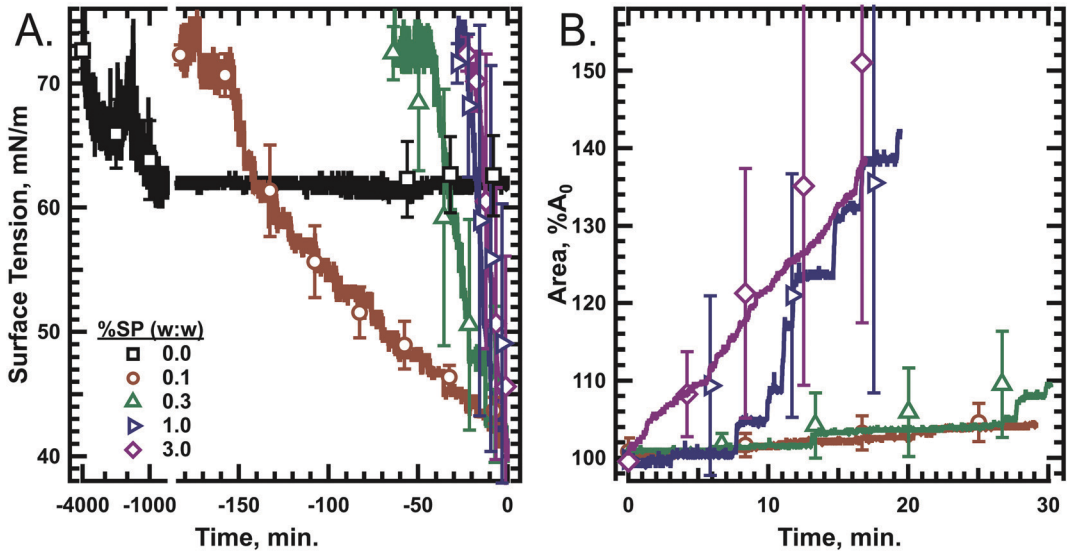

Fig. 7 Adsorption of DOPC with variable amounts of the SPs. (A) Initial adsorption to a surface with constant area. Time was set to zero at the end of this segment. The *x*-axis is split to display adsorption with different kinetics. (B) Subsequent isobaric adsorption, with the interface held at a surface tension of 40 mN m^{-1}. For both panels, symbols show mean ± S.D., while solid lines show a representative trace. $n \geq 4$. Temperature = 30 °C.

isobaric adsorption was considered zero. With the proteins present, the rate increased with greater amounts of the SPs (Fig. 7B).

The SPs with the surfactant lipids produced changes in adsorption (Fig. 8) similar to their effects on DOPC (Fig. 7), and a similar discrepancy with the results from XDS. N&PL alone failed to reach 40 mN m^{-1} during adsorption for 83 h (Fig. 8A). Samples at X_{CLSE} = 0.1 adsorbed to 40 mN m^{-1} (Fig. 8A), but the rate of isobaric expansion at that surface tension was minimal (Fig. 8B). Increasing X_{CLSE} to 0.3 and then 0.5 produced an incremental increase in the isobaric rate. The kinetics at X_{CLSE} = 0.5 approximated the rate for CLSE, indicating that the proteins achieved their maximal effect below physiological levels.

The dose–response for both lipids followed a sigmoidal trend, with lower concentrations of protein producing little effect at and below 0.3 wt% (Fig. 9A (DOPC) and B (N&PL/CLSE)). This behavior was different from the changes in S_{xray} and K_C produced by the proteins in both lipids.

4. Discussion

These studies concern one of the earliest models of how pulmonary surfactant functions in the lungs. The classical model proposes

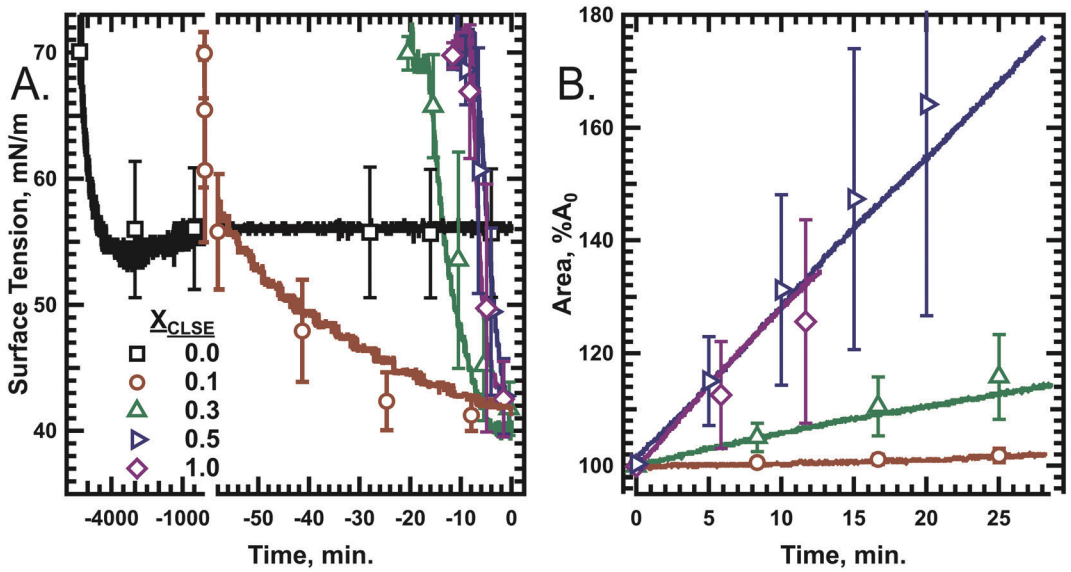

Fig. 8 Adsorption of surfactant lipids with variable amounts of the SPs. (A) Initial adsorption to a surface with constant area. (B) Subsequent isobaric adsorption, with the interface held at a surface tension of 40 mN m^{-1}. Details as in Fig. 7, except temperature = 40 °C.

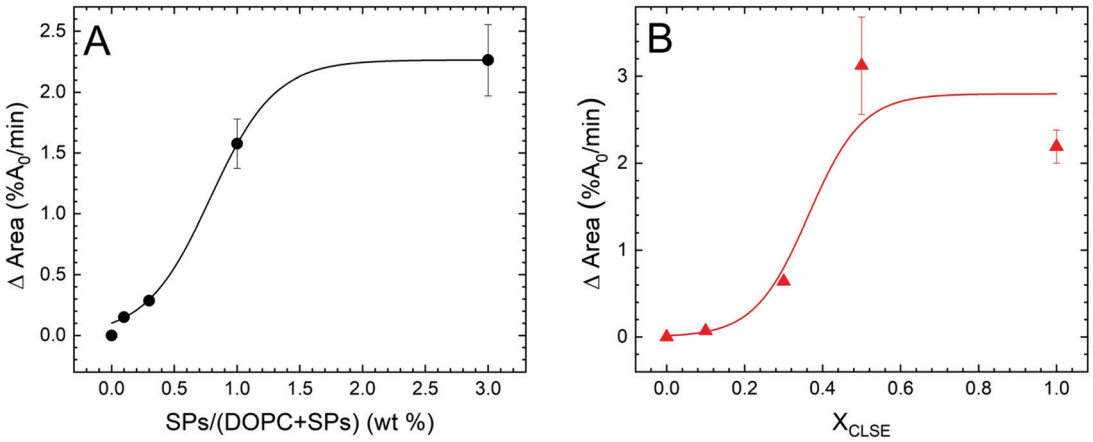

Fig. 9 Effects of the SPs on rates of isobaric adsorption at 40 mN m^{-1} (Fig. 7B and 8B). (A) DOPC. (B) N&PL/CLSE. Lines guide the eye. Symbols give mean ± S.D. $n \geq 4$.

that the alveolar film which sustains low surface tensions is an ordered structure containing mostly dipalmitoylphosphatidylcholine (DPPC). That compound represents the most prevalent constituent of pulmonary surfactant from most mammals.[61] DPPC by itself, however, adsorbs slowly.[62,63] Early investigators proposed that the other constituents generate disorder in the bilayers of the freshly secreted surfactant vesicles, making them more fluid, and allowing adsorption to proceed more rapidly.[15,64] This proposal preceded the discovery of the hydrophobic surfactant proteins, but it naturally extends to explain their essential role in promoting adsorption. The model leads directly to hypotheses concerning the mechanisms by which the proteins promote adsorption. They should disorder the surfactant lipids and decrease the rigidity of lipid leaflets, resulting in their kinetic effect.

Despite the early formulation of this model, these hypotheses have largely gone untested. The measurements of XDS here determine the effects of the proteins on both lipid-order and the bending modulus of lipid bilayers. Our experiments consider the dose–response of the proteins with both DOPC, used as a simple, well characterized model system, and the complete set of surfactant lipids. We then compare the effects of the proteins on adsorption with the changes determined by XDS. This comparison tests whether structural effects of the proteins, and the resultant changes in membrane-elasticity, correspond to functional changes in adsorption.

The effects of the proteins on S_{xray} and K_C agree well. These variables are determined independently from WAXS and LAXS, respectively. With both lipids, for all doses of the proteins, changes in S_{xray} shift K_C in the same direction. Loss of order in the lipids decreases the rigidity of the bilayers. The results are self-consistent and expected.

The values of S_{xray} also generally agree with expected behavior. Prior compositional determinations of the lipids in CLSE indicate that the phospholipid acyl chains are ~25% monounsaturated and ~75% saturated.[11] Values of S_{xray} obtained by adding cholesterol to pure lipids allows estimation of the order parameter for this composition.[47,48] These calculations indicate that N&PL should have $S_{xray} \approx 0.515$, close to our measured value of 0.5.

The dose-dependence of S_{xray} and K_C on the proteins, however, is dramatically different for the two lipids. With DOPC, the proteins produce a monotonic decrease in both variables. With the surfactant lipids, the change in these variables with increasing protein is reproducible, found with different samples during separate trips to CHESS, but erratic. Those changes correspond poorly to known structural alterations produced by the proteins with the surfactant lipids.[59] At 40 °C, WAXS from N&PL shows weak diffraction that suggests a correlation among the phospholipid headgroups.[59] Increasing amounts of the proteins, achieved by adding CLSE, diminished this signal monotonically. The progression and elimination of that structure corresponds poorly to the behavior of the bilayers shown here.

Similar variable behavior occurs in a different system. Increasing amounts of an exogenous antimicrobial peptide produces similarly irregular changes in the elasticity of lipids that mimic the membranes of Gram-negative bacteria.[37] Interactions of the peptide at increasing concentrations with different components of the mixed lipids may explain that variation. Aggregation of the proteins could also play a role.[65] Our results here provide no insights concerning whether similar variations of interactions between the SPs and the surfactant lipids cause the changes in K_C.

The correspondence between the variables obtained by XDS and the kinetics of adsorption for both lipids is poor. The proteins produce a well behaved variation of isobaric adsorption with both lipids. The lipids alone fail to reach the equilibrium spreading tension of ~25 mN m^{-1}. Small amounts of protein allow both lipids to lower surface tension further, but the rate of isobaric adsorption is minimal. For DOPC, levels of protein that dramatically soften the bilayer have little effect on the isobaric adsorption. The marked acceleration of adsorption by DOPC occurs at levels of protein where elasticity has leveled. For the surfactant lipids, the progressively faster adsorption produced by the proteins corresponds poorly with their variable effects on S_{xray} and K_C. The lack of correlation strongly suggests that facilitation of adsorption by the proteins is unrelated to their effects on chain-order and elasticity.

Adsorption of surfactant vesicles may occur by a process similar to the fusion of two bilayers. Vesicles insert into the air/water interface as complete packets.[66–68] The proteins that facilitate adsorption also promote the fusion of vesicles.[69,70] Highly curved structures proposed as intermediates that minimize exposure of hydrophobic groups to the aqueous environment during fusion[71] would provide the same advantage during adsorption.[72] The proposed intermediate involves both mean and Gaussian curvatures as prominent features. The bending energy required to form these structures would benefit from changes in spontaneous curvature of the leaflets, and in both K_C and the Gaussian modulus.[73] The proteins produce major changes in spontaneous curvature.[74] They also induce conversion of lamellar phospholipids to bicontinuous cubic phases.[75] This transition to structures with negative Gaussian curvature could reflect simply the change in spontaneous curvature, or a shift in the Gaussian modulus, which is experimentally inaccessible.[76] The poor correlation here between elasticity and adsorption suggests that softening of the bilayers does not explain the functional effect of the proteins. The change in the spontaneous curvature of the leaflets, and possibly a shift in the Gaussian modulus, represent more likely mechanisms.

5. Conclusions

Increasing concentrations of the SPs produce dose-related increases in the adsorption of both DOPC and the surfactant lipids. At a constant surface tension of 40 mN m^{-1}, the rate at which adsorption increases surface area shows a sigmoidal dependence on the content of protein. The greatest kinetic effect occurs when the protein/lipid ratio is roughly half of the physiological level. This behavior corresponds poorly with the dose-dependent effects of the proteins on the order of the lipid chains and the bending modulus. The lack of correlation suggests that the previously demonstrated effects of the proteins on curvature and the formation of structures with Gaussian curvature may represent a better explanation for the ability of the proteins to promote adsorption.

Author contributions

The authors had the following roles, defined by the Consortia Advancing Standards in Research Administration Information: Ryan Loney: investigation, formal analysis, methodology, resources. Bret Brandner: investigation, formal analysis. Maayan Dagan: data curation, formal analysis. Paige Smith: investigation. Megan Roche: data curation, formal analysis, writing-reviewing and editing. Jonathan Fritz: formal analysis, writing-reviewing and editing. Stephen Hall: conceptualization, data curation, formal analysis, funding acquisition, methodology, project administration, resources, supervision, validation, visualization, writing-reviewing and editing. Stephanie Tristram-Nagle: formal analysis, investigation, methodology, project administration, resources, software, supervision, validation, visualization, writing-original draft and reviewing and editing.

Conflicts of interest

There are no conflicts of interest to declare.

Acknowledgements

The authors thank Yasmene Elhady, Diamond Moody, Akari Kumagai, John Nagle and Horia Petrache for help with the collection of data at CHESS. Dr Arthur Woll from the G1 line at CHESS helped align the X-ray beam. Hannah Smith prepared the oriented samples of N&PL/CLSE for the second set of measurements. Dr Markus Deserno contributed the periodic minimal surface used to represent a bicontinuous cubic phase in the figure for the Table of Contents. These studies were supported by the National Institutes of Health (HL060914, HL130130, and HL136734). Measurements of XDS were performed at CHESS, which is supported by National Science Foundation (NSF) under award no. DMR-1332208.

References

1 J. Goerke and J. A. Clements, in *Handbook of Physiology – The Respiratory System. Vol. III, Part 1*, ed. P. T. Macklem and J. Mead, American Physiological Society, Washington, D.C., 1985, vol. III, pp. 247–261.
2 K. R. Melton, L. L. Nesslein, M. Ikegami, J. W. Tichelaar, J. C. Clark, J. A. Whitsett and T. E. Weaver, *Am. J. Physiol.*, 2003, **285**, L543–L549.
3 F. S. Cole, *Am. J. Physiol.*, 2003, **285**, L540–L542.
4 B. Robertson, in *Pulmonary Surfactant*, ed. B. Robertson, L. M. G. Van Golde and J. J. Batenburg, Elsevier Science Publishers, Amsterdam, 1st edn, 1984, pp. 383–418.
5 L. M. Nogee, *Annu. Rev. Physiol.*, 2004, **66**, 601–623.
6 L. M. Nogee, A. E. Dunbar, 3rd, S. E. Wert, F. Askin, A. Hamvas and J. A. Whitsett, *N. Engl. J. Med.*, 2001, **344**, 573–579.
7 L. M. Nogee and B. C. Trapnell, in *Kendig and Chernick's Disorders of the Respiratory Tract in Children*, ed. E. L. Kendig and R. W. Wilmott, Elsevier/Saunders, Philadelphia, PA, 8th edn, 2012, pp. 810–821.
8 R. S. Amin, S. E. Wert, R. P. Baughman, J. F. Tomashefski, Jr., L. M. Nogee, A. S. Brody, W. M. Hull and J. A. Whitsett, *J. Pediatr.*, 2001, **139**, 85–92.
9 S. W. Glasser, M. S. Burhans, T. R. Korfhagen, C. L. Na, P. D. Sly, G. F. Ross, M. Ikegami and J. A. Whitsett, *Proc. Natl. Acad. Sci. U. S. A.*, 2001, **98**, 6366–6371.
10 S. B. Hall, Z. Wang and R. H. Notter, *J. Lipid Res.*, 1994, **35**, 1386–1394.
11 M. C. Kahn, G. J. Anderson, W. R. Anyan and S. B. Hall, *Am. J. Physiol.*, 1995, **269**, L567–L573.
12 S. C. Biswas, S. B. Rananavare and S. B. Hall, *Biochim. Biophys. Acta*, 2005, **1717**, 41–49.
13 V. Schram and S. B. Hall, *Biophys. J.*, 2001, **81**, 1536–1546.
14 R. J. King and J. A. Clements, *Am. J. Physiol.*, 1972, **223**, 727–733.
15 J. A. Clements, *Am. Rev. Respir. Dis.*, 1977, **115**(6 part 2), 67–71.

16 R. H. Notter, J. N. Finkelstein and R. D. Taubold, *Chem. Phys. Lipids*, 1983, **33**, 67–80.
17 E. G. Bligh and W. J. Dyer, *Can. J. Biochem. Physiol.*, 1959, **37**, 911–917.
18 A. Takahashi and T. Fujiwara, *Biochem. Biophys. Res. Commun.*, 1986, **135**, 527–532.
19 S. Hawgood, B. J. Benson, J. Schilling, D. Damm, J. A. Clements and R. T. White, *Proc. Natl. Acad. Sci. U. S. A.*, 1987, **84**, 66–70.
20 S. G. Taneva, J. Stewart, L. Taylor and K. M. W. Keough, *Biochim. Biophys. Acta*, 1998, **1370**, 138–150.
21 R. S. Kaplan and P. L. Pedersen, *Anal. Biochem.*, 1985, **150**, 97–104.
22 B. N. Ames, *Methods Enzymol.*, 1966, **VIII**, 115–118.
23 M. van Eijk, C. G. De Haas and H. P. Haagsman, *Anal. Biochem.*, 1995, **232**, 231–237.
24 S. A. Tristram-Nagle, *Methods Mol. Biol.*, 2007, **400**, 63–75.
25 N. Kučerka, Y. Liu, N. Chu, H. I. Petrache, S. Tristram-Nagle and J. F. Nagle, *Biophys. J.*, 2005, **88**, 2626–2637.
26 Y. Liu and J. F. Nagle, *Phys. Rev. E: Stat., Nonlinear, Soft Matter Phys.*, 2004, **69**, 040901.
27 Y. Lyatskaya, Y. Liu, S. Tristram-Nagle, J. Katsaras and J. F. Nagle, *Phys. Rev. E: Stat., Nonlinear, Soft Matter Phys.*, 2001, **63**, 1–9.
28 Y. Liu, PhD thesis, Carnegie Mellon University, 2003.
29 S. Tristram-Nagle and J. F. Nagle, *Chem. Phys. Lipids*, 2004, **127**, 3–14.
30 J. Pan, S. Tristram-Nagle, N. Kučerka and J. F. Nagle, *Biophys. J.*, 2008, **94**, 117–124.
31 J. F. Nagle, M. S. Jablin, S. Tristram-Nagle and K. Akabori, *Chem. Phys. Lipids*, 2015, **185**, 3–10.
32 N. Chu, N. Kučerka, Y. Liu, S. Tristram-Nagle and J. F. Nagle, *Phys. Rev. E: Stat., Nonlinear, Soft Matter Phys.*, 2005, **71**, 041904.
33 A. L. Boscia, B. W. Treece, D. Mohammadyani, J. Klein-Seetharaman, A. R. Braun, T. A. Wassenaar, B. Klosgen and S. Tristram-Nagle, *Chem. Phys. Lipids*, 2014, **178**, 1–10.
34 S. D. Guler, D. D. Ghosh, J. Pan, J. C. Mathai, M. L. Zeidel, J. F. Nagle and S. Tristram-Nagle, *Chem. Phys. Lipids*, 2009, **160**, 33–44.
35 N. Kučerka, S. Tristram-Nagle and J. F. Nagle, *Biophys. J.*, 2006, **90**, L83–L85.
36 H. I. Petrache, S. Tristram-Nagle, K. Gawrisch, D. Harries, V. A. Parsegian and J. F. Nagle, *Biophys. J.*, 2004, **86**, 1574–1586.
37 F. G. Dupuy, I. Pagano, K. Andenoro, M. F. Peralta, Y. Elhady, F. Heinrich and S. Tristram-Nagle, *Biophys. J.*, 2018, **114**, 919–928.
38 S. Tristram-Nagle, *J. Phys. D: Appl. Phys.*, 2018, **51**, 183001.
39 C. Neale, K. Huang, A. E. Garcia and S. Tristram-Nagle, *Membranes*, 2015, **5**, 473–494.
40 K. Akabori, K. Huang, B. W. Treece, M. S. Jablin, B. Maranville, A. Woll, J. F. Nagle, A. E. Garcia and S. Tristram-Nagle, *Biochim. Biophys. Acta*, 2014, **1838**, 3078–3087.
41 A. L. Boscia, K. Akabori, Z. Benamram, J. A. Michel, M. S. Jablin, J. D. Steckbeck, R. C. Montelaro, J. F. Nagle and S. Tristram-Nagle, *Biophys. J.*, 2013, **105**, 657–666.
42 P. Shchelokovskyy, S. Tristram-Nagle and R. Dimova, *New J. Phys.*, 2011, **13**, 25004.
43 S. Tristram-Nagle and J. F. Nagle, *Biophys. J.*, 2007, **93**, 2048–2055.
44 A. I. Greenwood, J. Pan, T. T. Mills, J. F. Nagle, R. M. Epand and S. Tristram-Nagle, *Biochim. Biophys. Acta*, 2008, **1778**, 1120–1130.
45 S. Tristram-Nagle, R. Chan, E. Kooijman, P. Uppamoochikkal, W. Qiang, D. P. Weliky and J. F. Nagle, *J. Mol. Biol.*, 2010, **402**, 139–153.
46 N. Kučerka, J. D. Perlmutter, J. Pan, S. Tristram-Nagle, J. Katsaras and J. N. Sachs, *Biophys. J.*, 2008, **95**, 2792–2805.
47 J. Pan, S. Tristram-Nagle and J. F. Nagle, *Phys. Rev. E: Stat., Nonlinear, Soft Matter Phys.*, 2009, **80**, 021931.
48 J. Pan, T. T. Mills, S. Tristram-Nagle and J. F. Nagle, *Phys. Rev. Lett.*, 2008, **100**, 198103.
49 J. F. Nagle, M. S. Jablin and S. Tristram-Nagle, *Chem. Phys. Lipids*, 2016, **196**, 76–80.
50 M. F. Peralta, H. Smith, D. Moody, S. Tristram-Nagle and D. C. Carrer, *J. Phys. Chem. B*, 2018, **122**, 7332–7339.
51 M. Raghunathan, Y. Zubovski, R. M. Venable, R. W. Pastor, J. F. Nagle and S. Tristram-Nagle, *J. Phys. Chem. B*, 2012, **116**, 3918–3927.
52 T. T. Mills, G. E. Toombes, S. Tristram-Nagle, D. M. Smilgies, G. W. Feigenson and J. F. Nagle, *Biophys. J.*, 2008, **95**, 669–681.
53 J. D. Malcolm and C. D. Elliott, *Can. J. Chem. Eng.*, 1980, **58**, 151–153.
54 S. Schürch, H. Bachofen, J. Goerke and F. Possmayer, *J. Appl. Physiol.*, 1989, **67**, 2389–2396.
55 W. M. Schoel, S. Schürch and J. Goerke, *Biochim. Biophys. Acta*, 1994, **1200**, 281–290.
56 Y. Y. Zuo, M. Ding, D. Li and A. W. Neumann, *Biochim. Biophys. Acta, Gen. Subj.*, 2004, **1675**, 12–20.
57 E. C. Smith, J. M. Crane, T. G. Laderas and S. B. Hall, *Biophys. J.*, 2003, **85**, 3048–3057.
58 R. W. Loney, W. R. Anyan, S. C. Biswas, S. B. Rananavare and S. B. Hall, *Langmuir*, 2011, **27**, 4857–4866.
59 J. R. Fritz, R. W. Loney, S. B. Hall and S. Tristram-Nagle, *Biophys. J.*, 2021, **120**, 243–253.
60 R. D. Smith and J. C. Berg, *J. Colloid Interface Sci.*, 1980, **74**, 273–286.
61 A. D. Postle, E. L. Heeley and D. C. Wilton, *Comp. Biochem. Physiol., Part A: Mol. Integr. Physiol.*, 2001, **129**, 65–73.
62 L. W. Horn and N. L. Gershfeld, *Biophys. J.*, 1977, **18**, 301–310.
63 S. Lee, D. H. Kim and D. Needham, *Langmuir*, 2001, **17**, 5544–5550.
64 R. H. Notter, in *Pulmonary Surfactant*, ed. B. Robertson, L. M. G. van Golde and J. J. Batenburg, Elsevier, Amsterdam, 1984, pp. 17–64.
65 B. Olmeda, B. García-Álvarez, M. J. Gómez, M. Martínez-Calle, A. Cruz and J. Pérez-Gil, *FASEB J.*, 2015, **29**, 4236–4247.
66 A. Sen, S.-W. Hui, M. Mosgrober-Anthony, B. A. Holm and E. A. Egan, *J. Colloid Interface Sci.*, 1988, **126**, 355–360.
67 S. Schürch, D. Schürch, T. Curstedt and B. Robertson, *J. Appl. Physiol.*, 1994, **77**, 974–986.
68 T. Haller, P. Dietl, H. Stockner, M. Frick, N. Mair, I. Tinhofer, A. Ritsch, G. Enhorning and G. Putz, *Am. J. Physiol.*, 2004, **286**, L1009–L1015.
69 K. Shiffer, S. Hawgood, N. Duzgunes and J. Goerke, *Biochemistry*, 1988, **27**, 2689–2695.

70 F. R. Poulain, S. Nir and S. Hawgood, *Biochim. Biophys. Acta*, 1996, **1278**, 169–175.
71 V. S. Markin, M. M. Kozlov and V. L. Borovjagin, *Gen. Physiol. Biophys.*, 1984, **3**, 361–377.
72 R. W. Walters, R. R. Jenq and S. B. Hall, *Biophys. J.*, 2000, **78**, 257–266.
73 W. Helfrich, *Z. Naturforsch.*, 1973, **28**, 693–703.
74 M. Chavarha, R. W. Loney, S. B. Rananavare and S. B. Hall, *Biophys. J.*, 2015, **109**, 95–105.
75 M. Chavarha, R. W. Loney, K. Kumar, S. B. Rananavare and S. B. Hall, *Langmuir*, 2012, **28**, 16596–16604.
76 M. Deserno, *J. Phys. D: Appl. Phys.*, 2018, **51**, 343001.